

ORIGINAL ARTICLE

Drug susceptibility profile and pathogenicity of H7N9 influenza virus (Anhui1 lineage) with R292K substitution

Xiaonan Zhang^{1,*}, Zhigang Song^{1,*}, Jing He^{1,*}, Hui-Ling Yen^{2,*}, Jianhua Li³, Zhaoqin Zhu¹, Di Tian¹, Wei Wang¹, Lei Xu¹, Wencai Guan¹, Yi Liu¹, Sen Wang^{1,3}, Bisheng Shi¹, Wanju Zhang¹, Boyin Qin⁴, Jialin Cai⁴, Yanmin Wan⁵, Chunhua Xu⁴, Xiaonan Ren⁴, Haili Chen¹, Lu Liu⁵, Yuqin Yang⁴, Xiaohui Zhou⁴, Wenjiang Zhou⁴, Jianqing Xu^{3,5}, Xiaoyan Zhang^{3,5}, Malik Peiris², Yunwen Hu¹ and Zhenghong Yuan³

Neuraminidase inhibitors (NAIs) are the only available licensed therapeutics against human H7N9 influenza virus infections. The emergence of NAI-resistant variants of H7N9 viruses with an NA R292K mutation poses a therapeutic challenge. A comprehensive understanding of the susceptibility of these viruses to clinically available NAIs, non-NAIs and their combinations is crucial for effective treatment. In this study, by using limited serial passage and plaque purification, an R292K variant of the Anhui1 lineage was isolated from a patient with clinical evidence of resistance to oseltamivir. *In vitro* and cell-based assays confirmed a high level of resistance conferred by the R292K mutation to oseltamivir carboxylate and a moderate level of resistance to zanamivir and peramivir. Non-NAI antivirals, such as T-705, ribavirin and NT-300, efficiently inhibited both the variant and the wild-type in cell-based assays. A combination of NAIs and non-NAIs did not exhibit a marked synergistic effect against the R292K variant. However, the combination of two non-NAIs (T-705 and ribavirin) exhibited significant synergism against the mutant virus. In experimentally infected mice, the variant showed delayed onset of symptoms, a reduced viral load and attenuated lethality compared with the wild-type. Our study suggested non-NAIs should be tested clinically for H7N9 patients with a sustained high viral load. Possible drug combination regimens, such as T-705 plus ribavirin, should be further tested in animal models. The pathogenicity and transmissibility of the R292K H7N9 variant should be further assessed with genetically well-characterized pairs of viruses and, most-desirably, with competitive fitness experiments.

Emerging Microbes and Infections (2014) 3, e78; doi:10.1038/emi.2014.80; published online 12 November 2014

Keywords: H7N9; influenza virus; neuraminidase; oseltamivir; peramivir

INTRODUCTION

A novel H7N9 avian influenza virus infecting humans in eastern China was first reported on 30 March 2013.¹ The epidemic curve of the first wave of human infection spanned the period from mid-February to the end of May 2013, and comprised 132 human infections with a case fatality rate of 28%. The second wave of human infections from the winter of 2013 to the spring of 2014 resulted in over 200 confirmed cases.

Phylogenetic and evolutionary analyses of isolates from wild and domestic birds collected from 2009 to 2013 suggested that the novel avian H7N9 influenza virus arose from sequential reassortments in domestic poultry involving distinct H9N2 donor viruses as well as distinct H7 and N9 precursors in wild birds.^{2,3} Clinical isolates from this epidemic were found to form two separate subclades. The dominant genotype is that of the A/Anhui/1/2013 (Anhui1) lineage and the minor one is represented by only two reported isolates: A/Shanghai/1/2013 (Shanghai1)⁴ and A/Shanghai/05/2013 (H7N9)⁵ (also reported as A/Shanghai/JS01/2013 (H7N9)⁶).

The initial sequence analysis of Shanghai1 revealed that its neuraminidase (NA) protein has an R292K (N2 numbering) mutation,¹ which has been reported to confer resistance to NA inhibitors (NAIs).^{7,8} Further investigation indicated that the clinical isolate of Shanghai1 was a mixed population containing either arginine or lysine at residue 292 of the NA. Plaque purification of clones containing NA^{K292} confirmed its resistance phenotype against NAIs.⁹ We and others reported that this mutation emerged in H7N9 patients receiving NAI treatment.^{10,11} Furthermore, the emergence of the R292K mutation was accompanied by prolonged virus shedding and adverse clinical outcomes in two patients.¹⁰ Of note, the viral isolates obtained from these patients are of the Anhui1 lineage (data not shown), which is distinct from the previously characterized Shanghai1 virus with multiple amino-acid differences within the receptor binding site of hemagglutinin (HA) (A138, V186 and L226 in Anhui1-like viruses, S138, G186 and Q226 in Shanghai1 virus).^{4,12} As the changes in the HA receptor binding domain may affect the HA binding affinity or specificity, the above mentioned amino

¹Department of Pathogen Diagnosis and Biosafety, Shanghai Public Health Clinical Center, Fudan University, Shanghai 201508, China; ²State Key Laboratory of Emerging Infectious Disease, School of Public Health, University of Hong Kong, Hong Kong, China; ³Key Lab of Medical Molecular Virology, School of Basic Medical Science, Fudan University, Shanghai 200032, China; ⁴Animal Center, Shanghai Public Health Clinical Center, Fudan University, Shanghai 201508, China and ⁵Scientific Research Center, Shanghai Public Health Clinical Center, Fudan University, Shanghai 201508, China

*These authors contributed equally to this work.

Correspondence: YW Hu; ZH Yuan

E-mail: ywhu@shaphc.org; zhyuan@shaphc.org

Received 13 August 2014; revised 21 September 2014; accepted 22 September 2014

acid differences between Anhui1 and Shanghai1 may influence viral dependence on NA activity and sensitivity to NAIs. Therefore, further comprehensive analysis of the R292K mutant virus from this clinically dominant Anhui1 subclade is necessary to further understand the resistance spectrum, viral fitness and pathogenesis and to explore possible therapeutic options for the control of this clinically challenging variant. In the present study, we obtained an R292K mutant virus derived from an H7N9 (Anhui1 lineage)-infected patient in whom we observed a sustained high viral load despite continued NAI treatment. The mutant virus's drug resistance profile and the pathogenesis of infection in the mouse model were investigated in parallel with those of its wild-type counterpart.

MATERIALS AND METHODS

Virus, compounds and reagents

All viruses were isolated and passaged in Madin–Darby canine kidney (MDCK) cells (ATCC). A/Shanghai/2167/2010(H1N1) was isolated from a patient infected with 2009 pdmH1N1 influenza virus. A/Shanghai/5190/2013(H7N9) (denoted SH5190) was isolated from patient number two described in our previous report, on day 8 post NAI treatment.¹⁰ The patient started oseltamivir treatment (150 mg twice daily) on day 6 post disease onset and switched to peramivir (0.6 g once daily) on day 10 post disease onset (days 10–16). However, persistent virus shedding was observed in serial nasopharyngeal samples despite continuous treatment with oseltamivir and peramivir. He developed severe acute respiratory distress syndrome and died at day 19 after disease onset. An R292K mutation was later found in throat swab samples starting from day 4 after oseltamivir treatment using genotypic analysis. The R292K variant (SH5190 R292K) was derived after serial passages and plaque purification. The genome sequences of SH5190 R292K (KF997839–KF-997846) and SH5190 wild-type (KF997831–KF997838) are available at NCBI. All experiments were performed in a biosafety level 3 laboratory at the Shanghai Public Health Clinical Center. Three clinically available NAIs were included in our study: oseltamivir, peramivir and zanamivir. Oseltamivir carboxylate was provided by Hoffmann La-Roche (Basel, Switzerland). Peramivir and zanamivir were purchased from Selleck Chemicals (Houston, TX, USA). These compounds were dissolved in deionized water and diluted for enzyme-based and cell-based assays. Three non-NAIs, including favipiravir (T705), nitazoxanide (NT-300) and ribavirin, were purchased from Sigma-Aldrich, Inc. (St Louis, MO, USA) and were dissolved in DMSO. Exogenous bacterial neuraminidase derived from *Clostridium perfringens* were purchased from Sigma-Aldrich, Inc.

Enzyme-based NA inhibition assay

The susceptibility of H7N9 viruses to oseltamivir carboxylate, zanamivir and peramivir was determined by the NA-StarTM Influenza Neuraminidase Inhibitor Resistance Detection Kit (Applied Biosystems, Foster City, CA, USA) according to the manufacturer's instructions. The chemiluminescent signal was measured with a Victor 1420 multi-label counter (PerkinElmer, Waltham, MA, USA).

Plaque reduction assay

Confluent MDCK cells in six-well plates were infected with SH5190 or SH5190 R292K and diluted to 100 plaque forming unit (PFU) per well in dulbecco's modified eagle medium (DMEM). After 1-h adsorption, media were replaced with DMEM containing 1 µg/mL tosyl phenylalanyl chloromethyl ketone (TPCK)-trypsin, 1% agarose and oseltamivir carboxylate at specified concentrations. Cells were subsequently cultured for three days and the plaques were fixed in 10% neutral

formaldehyde overnight and stained with 0.5% crystal violet; plaque diameters were measured. These experiments were repeated twice.

RNA extraction and quantitative real-time polymerase chain reaction (qRT-PCR)

Viral RNAs were extracted using a QIAamp Viral RNA Mini Kit (Qiagen, Valencia, CA, USA) from a 140 µL volume specimen. Viral load was measured by a TaqMan Real-time quantitative PCR assay using a one-step RT-PCR kit (TaKaRa Bio, Shiga, Japan). A pair of in-house designed primers and a probe (forward primer: 5'-GAA GAG GCA ATG CAA AAT AGA ATA CA-3', reverse primer: 5'-CCC GAA GCT AAA CCA RAG TAT CA-3' and probe: FAM5'-CCA GTC AAA CTA AGC AGY GGC TAC AAA-3'BHQ) that specifically amplify a fragment of HA gene influenza A subtype H7 virus were used. A TaqMan single nucleotide polymorphisms (SNPs) assay for detecting the NA R292K oseltamivir-resistance mutation was established,¹³ with primers (forward: 5'-CAT GTT ACG GGR ARC GAA CAG G-3', reverse: 5'-TGG TCT ATT TGA GCC CTG CC A-3'), and probes (K292: FAM5'-CAC ATG CAA GGA CAA-3'MGB; R292: VIC5'-CAC ATG CAG GGA CAA-3'MGB).

Virus yield reduction assay

The sensitivity of the wild-type and the R292K variant to NAIs and non-NAIs were evaluated in MDCK cells against the following ranges of drugs: oseltamivir carboxylate (0.03–100 µM for wild-type, 0.3–1000 µM for mutant), peramivir (0.03–100 µM for wild-type, 0.3–1000 µM for mutant), zanamivir (0.03–100 µM for wild-type, 0.23–500 µM for mutant), ribavirin (0.03–100 µM), NT-300 (0.03–100 µM) and T705 (0.03–100 µM). Briefly, confluent cells in 96-well plates were inoculated with SH5190 or SH5190 R292K diluted in DMEM (50 PFU/well) at 37 °C for 1 h. The culture medium was then replaced with DMEM containing 1 µg/mL TPCK-trypsin and antiviral compounds diluted to various concentrations in triplicate. Supernatants were collected 24 h post infection and influenza HA gene copy numbers were quantified using one-step qRT-PCR. In some experiments, supernatants were collected 48 h post infection and were titrated in MDCK cells to determine viral titers (log₁₀ TCID₅₀/mL). These experiments were repeated at least twice. The 50% inhibitory concentration (IC₅₀) value of each drug was estimated using non-linear regression functionality in GraphPad 5.0 with a variable slope and least-square fit method. The 95% confidence interval of IC₅₀ value was obtained after nonlinear regression to reflect the reliability of the estimate.

Viral replication kinetics

Confluent MDCK cells in six well plates were infected with SH5190 or SH5190 R292K at a multiplicity of infection (MOI) of 0.001 PFU per cell. Supernatants were collected at 0, 6, 12, 24, 36, 48 and 72 h post infection. Viral titers (log₁₀ TCID₅₀/mL) in the supernatants were determined by a 50% tissue culture infective dose (TCID₅₀) assay. The positivity of each well was determined by a hemagglutination assay using guinea pig red blood cells.

Analysis of drug synergism

MDCK cells were infected with SH5190 R292K or SH5190 at an MOI of 0.001 and were overlaid with medium containing oseltamivir carboxylate, zanamivir, peramivir, T705, ribavirin and NT-300 alone or in combination (as indicated) at fixed molar ratios (for SH5190 R292K: T-705/zanamivir=1:3, ribavirin/zanamivir=1:4, NT-300/zanamivir=1:20, T-705/peramivir=1:9, ribavirin/peramivir=1:9, NT-300/peramivir=1:60, NT-300/ribavirin=1:5, T705/ribavirin=4:5, T-705/NT-300=4:1; for SH5190 wild-type:T-705/OC=25:3,

ribavirin/OC=9:1, NT-300/OC=1:3, T-705/zanamivir=25:4, ribavirin/zanamivir=27:4, NT-300/zanamivir=1:4, T-705/peramivir=250:6, ribavirin/peramivir=270:6, NT-300/peramivir=5:3, NT-300/Ribavirin=1:27, T705/Ribavirin=25:27, T-705/NT-300=25:1). Supernatants were collected 24 h post infection and viral HA gene copy numbers were quantified using qRT-PCR. The combination index (CI) was calculated by the Chou–Talalay method.¹⁴ The Chou–Talalay method ‘is based on the median-effect equation, derived from the mass-action law principle, which is the unified theory that provides the common link between single entity and multiple entities, and first order and higher order dynamics’.¹⁵ This method recommends the constant-ratio drug combinations (at the $(IC_{50})_1/(IC_{50})_2$) based on the notion that the mixture can be deemed as a third drug. The dose–response curve and accompanying parameters for the mixture can therefore be obtained. For a certain response rate, the CI value is $((D)_1/(Dx)_1) + ((D)_2/(Dx)_2)$, where Dx is for the drug alone that inhibits a system $x\%$ and $(D)_1 + (D)_2$ in combination also inhibit $x\%$. A CI of <1 indicates synergism (CI values are interpreted as follows: <0.1 , very strong synergism; $0.1–0.3$, strong synergism; $0.3–0.7$, synergism; $0.7–0.85$, moderate synergism; and $0.85–0.90$, slight synergism). A CI of 1, or close to 1, indicates additive effects, and a CI of >1 indicates antagonism.

Pathogenicity in the mouse model

Six- to eight-week-old female C57BL/6 mice were purchased from B&K Universal Group (Shanghai, China) and were housed under specific pathogen free conditions at the animal facility of the Shanghai Public Health Clinical Center, Fudan University. Mice ($n=16–18$) were inoculated intranasally with 10^3 or 10^5 PFU of SH5190 or SH5190 R292K in 50 μ L phosphate buffered saline (PBS) under isoflurane anesthesia. Their body weight, clinical signs and survival were measured daily for 15 days. In compliance with animal ethics, mice with weight loss over 30% or with an obvious dying condition were euthanized. The survival experiments were repeated twice. Three mice in each group were sacrificed at days 3, 8 and 11 post infection and their lungs, livers, hearts and brains were collected for viral titration. The right or left lung lobes were mechanically homogenized in sterile PBS and stored in -80°C until use. Lung tissues collected at day 8 post infection were fixed in 4% paraformaldehyde, dehydrated, embedded in paraffin and cut into 5- μ m-thick sections, which were stained with hematoxylin and eosin. The slides were viewed using an Olympus BX51 microscope, and the images were captured and analyzed by the corresponding acquisition software (DP controller; Olympus, Tokyo, Japan). All mouse experimental procedures were approved by the animal ethics committee of the Shanghai Public Health Clinical Center.

Statistical analysis

All statistical analyses were performed using GraphPad Prism 5.0 (Graphpad, La Jolla, CA, USA). The Mann–Whitney U test was used to compare viral titers and animal weight loss. The mortality rates of different virus challenge groups were assessed by the Kaplan–Meier method.

RESULTS

Isolation of oseltamivir-resistant H7N9 clinical variant of the Anhui lineage

In a previous report, we identified the rapid emergence of oseltamivir resistant variants in two severe cases of H7N9 influenza infection. Sustained viral shedding was accompanied by the rapid emergence of the NA R292K quasispecies.¹⁰ A virus isolate, A/Shanghai/5190/2013(H7N9) (denoted SH5190), was cultured from nasopharyngeal specimens collected on day 8 post NAI treatment from patient number

two as reported previously, an 88-year-old male who died of H7N9 influenza-induced acute respiratory distress syndrome and multiple organ failure. The presence of the R292K mutant was identified in the mixed population at a proportion of 77%, by Taqman SNP assay (data not shown). However, after one blind passage of the nasopharyngeal specimen in MDCK cells, Taqman SNP analysis showed that the wild-type 292R became dominant (100%). We hypothesized that the low NA activity possessed by the R292K variant might render the mutant strain less competent at competing with the wild-type virus. To isolate the R292K variant, limited serial passages in the presence of an ascending concentration of oseltamivir carboxylate (from 10 μ M to 500 μ M) and exogenous neuraminidase (2 mU/mL) were performed. The R292K variant was successfully isolated under these conditions.

We then performed plaque purification to isolate individual clones from the isolate. Four mutant clones were selected and the full genome was analyzed by Sanger sequencing. Among them, clone 27 had no additional mutations other than NA R292K and HA R220G (H3 numbering) (data not shown). No additional mutations in all eight gene segments were observed (data not shown). Moreover, we did not observe any reversion of the R292K mutation to wild-type 292R in the absence of oseltamivir or exogenous NA during subsequent experiments, as evidenced by both Sanger sequencing and Taqman SNP qPCR assay. This result suggested that the R292K mutation can be stably maintained in cell culture. Thus, clone 27 (named SH5190 R292K) exhibited minimum adaptive mutation and was chosen in conjunction with SH5190 for further study.

Replication of the SH5190 wild-type and mutant viruses in MDCK cells

We first compared the proliferative property of SH5190 and the R292K variant in cell culture. As shown in Figure 1, SH5190 R292K replicated to comparable titers as the wild-type counterpart in multi-cycle replication conditions in MDCK cells. The titers of the SH5190 R292K were even higher than those of the wild-type SH5190 at 12 h ($P<0.05$). The plaque morphology showed no significant difference between the mutant and the wild-type in the absence of oseltamivir carboxylate (Figure 2). We thus concluded that the R292K mutant virus can propagate efficiently in cell culture.

Sensitivity of SH5190 and SH5190 R292K to oseltamivir carboxylate in plaque reduction assay

The significant difference in oseltamivir sensitivity between SH5190 and SH5190 R292K was first confirmed by a plaque reduction assay

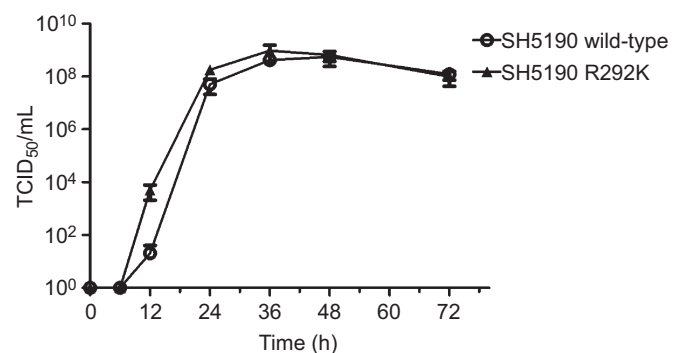


Figure 1 Replication kinetics of the wild-type virus and the R292K variant in MDCK cells. Confluent MDCK cells were infected with an MOI of 0.001 PFU per cell. Supernatants were collected at the time points indicated and titrated in MDCK cells using a TCID₅₀ assay. Each data point represents the log₁₀ mean \pm SEM TCID₅₀/mL from three replicated wells. The experiments were repeated twice.

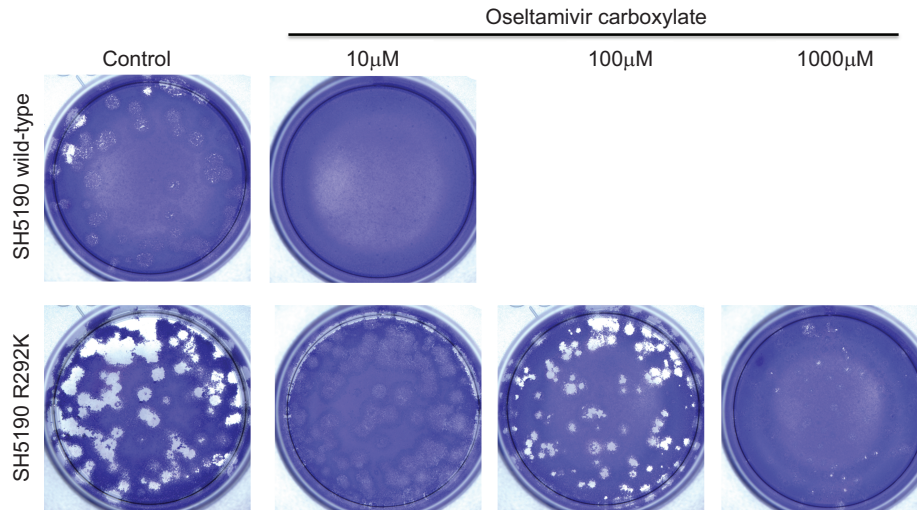


Figure 2 Plaque morphology of the wild-type (SH5190) and the R292K variant (SH5190 R292K) in the absence or presence of oseltamivir carboxylate (10–1000 μM).

under increasing concentration of oseltamivir carboxylate. As shown in Figure 2, the plaque size of the SH5190 was significantly reduced in the presence of 10 μM oseltamivir carboxylate (mean diameter <0.1 mm) when compared to the no drug control (mean diameter = 1.5 mm). In contrast, the plaque size of SH5190 R292K was not significantly affected in the presence (mean diameter = 1.8 mm) or absence (mean diameter = 1.8 mm) of 10 μM oseltamivir carboxylate. Only at 100 μM (mean diameter = 1.0 mm) or 1000 μM (mean diameter = 0.8 mm) of oseltamivir carboxylate was there notable plaque size reduction for SH5190 R292K, which indicated the highly resistant phenotype to oseltamivir.

Sensitivity of SH5190 and SH5190 R292K to NAIs in enzyme inhibition assay

The sensitivity of the SH5190 and SH5190 R292K to NAIs was further confirmed using enzymatic methods. The NA-Star assay was applied to determine the IC_{50} of NA enzymatic activity of SH5190 and SH5190 R292K in the presence of three clinically available NAIs: oseltamivir carboxylate, zanamivir and peramivir. A 2009pdmH1N1 virus isolate A/Shanghai/2167/2009 (denoted 2167) was included as a control. As shown in Table 1 and Figure 3, the wild-type virus is highly susceptible to all three NAIs, with IC_{50} values of 0.28 nM (peramivir), 0.48 nM (oseltamivir carboxylate) to 0.74 nM (zanamivir). However, SH5190 R292K exhibited a highly reduced susceptibility to oseltamivir carboxylate ($\text{IC}_{50} > 1000$ nM), which was out of the range of drug concentrations used for the assay. Its sensitivities to zanamivir (IC_{50} : 12.4 nM, 16.7-fold change) and peramivir (IC_{50} : 96.5 nM, 344-fold change) were also significantly reduced.

Table 1 IC_{50} value of the neuraminidase inhibitor in NA-star assay

	IC_{50} value (nM) [mean (95% CI)]		
	Oseltamivir carboxylate	Zanamivir	Peramivir
SH5190	0.48 (0.42–0.54)	0.74 (0.59–0.94)	0.28 (0.25–0.30)
SH5190 R292K	>1000	12.4 (9.67–15.9)	96.5 (10.2–91.1)
2167	1.96 (0.16–2.34)	0.18 (0.13–0.24)	0.11 (0.11–0.12)

Oseltamivir carboxylate

Sensitivity of SH5190 and SH5190 R292K to NAIs and non-NAIs in virus yield reduction assay

Next, we analyzed the sensitivity of SH5190 and SH5190 R292K against available NAIs and non-NAIs in a cell-based virus yield reduction assay. As expected, oseltamivir carboxylate exhibited a poor inhibitory effect against SH5190 R292K ($\text{IC}_{50} > 1000$ μM , Figure 4 and Table 2). Zanamivir and peramivir moderately inhibited viral growth with IC_{50} values of 33.5 μM and 898 μM , respectively. In contrast, the wild-type virus is fully susceptible to all three NAIs with IC_{50} at sub-micromolar values (oseltamivir carboxylate 0.37 μM , zanamivir 0.51 μM , peramivir 0.07 μM). Considering the adverse clinical outcome associated with the emergence of the NA R292K mutation after receiving NAI treatment, there is a pressing need to evaluate alternative therapeutic options to control this mutant virus. To this end, we performed a cell-based assay to evaluate the inhibition of virus replication by three non-NAIs, T-705 (favipiravir), ribavirin and NT-300 (nitazoxanide), on the wild-type and the R292K mutant. We observed that SH5190 and the R292K mutant exhibited comparable sensitivity to T-705 (IC_{50} values of 3.10 μM and 6.26 μM , respectively) and ribavirin (IC_{50} values of 3.32 μM and 7.43 μM , respectively). NT-300 was found to be over 25 times more potent than T-705 and ribavirin, with IC_{50} values of 0.12 μM to the wild-type (Figure 3 and Table 2). However, a greater than one log increase of IC_{50} in SH5190 R292K was observed for NT-300 (IC_{50} values of 1.60 μM).

Evaluation of drug combinations on the R292K mutant virus

Combination therapy with drugs targeting different viral proteins may reduce the emergence of drug-resistant mutants and may show synergistic inhibitory effects. For this consideration, we further investigated if the combinations of non-NAIs (T705, ribavirin or NT-300) with zanamivir or peramivir, which retained partial inhibitory activity against the R292K mutant virus, and combination between non-NAIs, may act synergistically to suppress growth of the R292K variant. We adopted the method of Chou and Talalay¹⁴ and computed the CI based on the data from cell-based experiments. For comparison, drug combinations were also tested on the wild-type virus. As shown in Supplementary Table S1, we observed six pairs of drug combinations (ribavirin + zanamivir; T-705 + zanamivir; NT-300 + peramivir; ribavirin + peramivir; T-705 + peramivir and NT-300 + ribavirin) that can achieve synergism at both IC_{50} and 90% inhibitory concentration

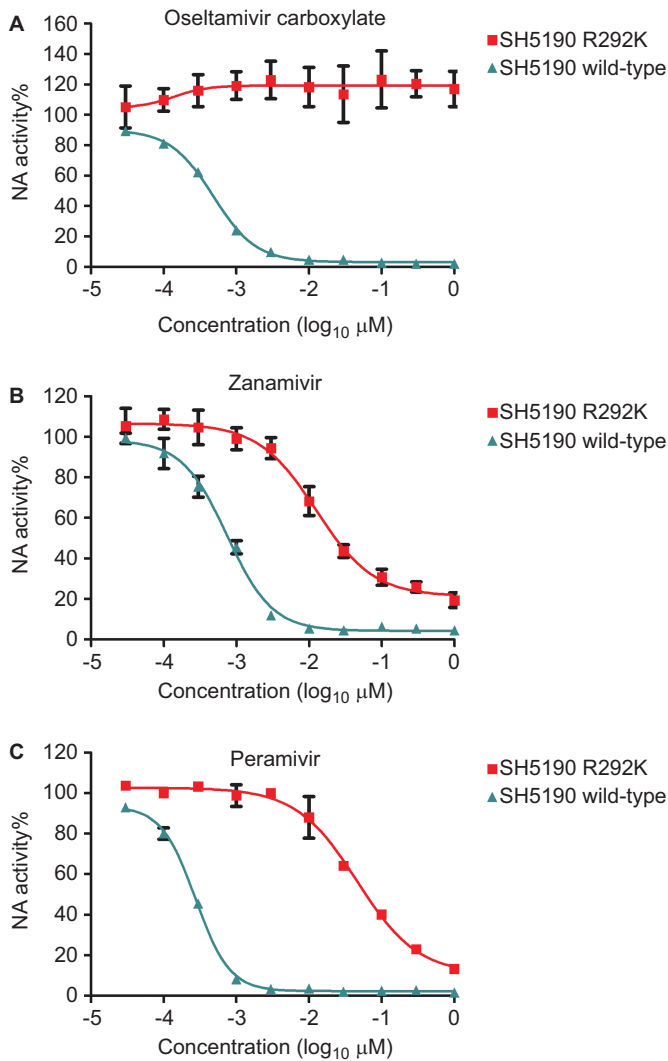


Figure 3 Dose–response curve of the SH5190, SH5190 R292K and the A(H1N1)pdm09 (2167) viruses in the presence of oseltamivir carboxylate (A), zanamivir (B) and peramivir (C) using a chemiluminescent (NA-star) assay. The NA activity of the H7N9 or H1N1 viruses under increasing concentrations (0.03–1000 nM) of the NAIs was determined. Each data point represents the normalized mean ± SEM neuraminidase activity from three replicated wells. The experiments were repeated twice.

(IC₉₀). For the R292K mutant, however, all combinations among NAIs and non-NAIs exhibited antagonism largely or merely additive effects at IC₅₀ (Table 3), which may be because the mutant virus is partially resistant to both zanamivir and peramivir. A marginal synergistic effect can only be observed at IC₉₀s in three combinations (T705+zanamivir CI=0.717, NT-300+peramivir CI=0.700, ribavirin+peramivir CI=0.444). For combinations of non-NAIs, moderate synergism was observed for NT-300+Ribavirin at IC₅₀ (CI=0.852). Of note, consistent synergism at IC₅₀ and IC₉₀ was only observed in the combination of T-705 and ribavirin (CI at IC₅₀=0.732, CI at IC₉₀=0.578; Table 3).

Pathogenesis of R292K mutant virus in experimentally infected mice

To gain a better understanding of the pathogenesis of the wild-type and mutant H7N9 virus *in vivo*, C57BL/6 mice were intranasally

inoculated with either SH5190 or SH5190 R292K at 10⁵ PFU (high dose group) or 10³ PFU (low dose group) and were monitored for 15 days. As reported previously, C57BL/6 mice infected with the H7N9 virus developed ruffled fur and difficulty in breathing, decreased their food and water intake and had obvious weight loss.¹⁶ However, the wild-type and the R292K variant showed an apparent difference in virus induced morbidity. As shown in Figure 5A, SH5190 R292K-infected mice exhibited a significant delay in weight loss compared to mice infected with the wild-type strain (Figure 5A). The difference between the wild-type and the R292K mutant was best exemplified at day 5 after infection in the high ($P<0.0001$, Mann–Whitney *U* test) dose group. Viral loads in mouse lungs were quantified using one-step qRT-PCR with RNA derived from homogenized mouse lungs collected at days 3, 8 and 11 post inoculation. The R292K variant was observed to replicate less efficiently than the wild-type at day 3 post inoculation (2.32 versus 3.49 log₁₀copy/μg RNA, $P=0.05$, Mann–Whitney *U* test). However, the viral loads of the two viruses were not significantly different at days 8 and 11 post infection (Figure 5B). The difference between SH5190 and SH5190 R292K in mouse lung titers is consistent with the trend in weight loss (Figure 5A) and the lethality of the viruses in mice (Figure 5C). Mice inoculated with a high dose of the wild-type virus resulted in a 45.5% (5/11) survival, whereas 90.9% (10/11) of the mice survived after infection with the same dose of the R292K variant after 15 days of observation ($P=0.018$) (Figure 5C).

Hematoxylin and eosin staining of lung tissues collected 8 days post infection also exhibited a different degree of pulmonary damage and inflammation. In SH5190 R292K-infected lungs, the alveolar septum was slightly thickened with the infiltration of inflammatory cells. The alveolar space was diminished and the serosity and inflammatory cell exudation were observed only in part of the pulmonary alveoli (Figures 6A and 6B). In comparison, eight days after SH5190 infection already resulted in diffused serosity and inflammatory cell (monocytes, macrophages and lymphocytes) exudation in most alveoli (Figures 6C and 6D), which seriously compromised the gas exchange efficiency. Of note, we did not detect a reversion of the R292K mutation back to the wild-type in the lungs of mice inoculated with SH5190 R292K during the observation period; in parallel, no R292K mutation was found in mice inoculated with the wild-type virus, as evidenced by the SNP qPCR assay (data not shown).

DISCUSSION

In contrast to previous zoonotic H7 influenza infections that rarely caused lethal infections in humans, the novel H7N9 avian influenza virus first reported in eastern China in March 2013 can cause severe pneumonia and acute respiratory distress syndrome) with a case fatality rate over 28%.^{1,17} It is disturbing that H7N9 infections may not always be effectively treated with oseltamivir, even when treatment is started early because of the emergence of resistant variants that lead to adverse clinical outcomes.^{10,18} We recently reported the emergence of the R292K mutation in the NA segment in two H7N9 fatal cases during NAI treatment.¹⁰ Thus, it is of clinical and scientific importance to characterize R292K variants of the dominant Anhui1 lineage (the dominant H7N9 virus lineage) from clinical specimens. Previous reports have generated a drug-resistant virus by introducing a Shanghai1 NA segment with a 292K mutation into a Anhui1 gene frame using reverse genetics.¹⁹ To make an NAI-resistant strain, we report here the isolation of the R292K mutant virus of Anhui1 lineage without genetic manipulation. This R292K variant derived from a clinical specimen is critical to confirm the results derived from recombinant viruses and to investigate potential antiviral strategies to inhibit the NAIs-resistant strain.

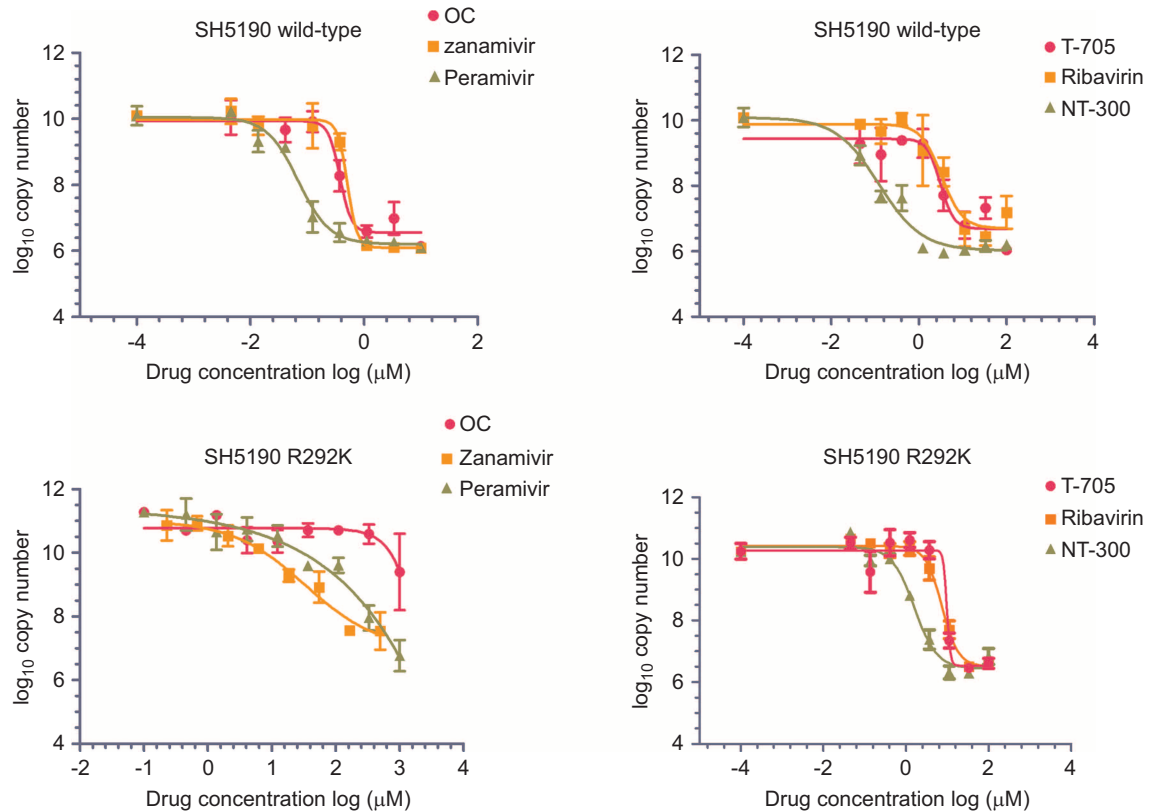


Figure 4 The sensitivity of the wild-type and the R292K virus to oseltamivir carboxylate, zanamivir, peramivir, T705, ribavirin and NT-300 in MDCK cells. MDCK cells were infected with the wild-type or R292K variant at a dose of 50 PFU/well and were incubated at 37 °C for 1 h, after which the inoculum was removed. Antiviral compounds were diluted to specified concentrations, added in the culture and incubated at 37 °C. Supernatants were collected 24 h post infection and viral loads under different antiviral compounds were quantified using qRT-PCR to determine the influenza A virus HA gene copy numbers. Each data point represents the mean \pm SEM of \log_{10} copy number from three replicated wells. The experiments were repeated at least three times.

Interestingly, we had difficulty isolating the R292K variant *in vitro* under oseltamivir carboxylate selection pressure alone (data not shown). The addition of exogenous NA from *Clostridium perfringens* greatly facilitated this process, possibly because of the low NA activity exhibited by the R292K variants.^{9,20} Nevertheless, the R292K variant that we obtained through plaque purification efficiently replicated in MDCK cells when exogenous NA was withdrawn (Figures 1 and 2). We speculate that the R292K mutation caused subtle changes in the activity of neuraminidase, which may need some compensatory intermediate mutations in the NA and/or HA segment. The exogenous NA from *Clostridium perfringens* might facilitate this process. Full genome sequencing showed that in addition to the R292K mutation in the NA gene, this variant as only one amino acid substitution (R220G) in the proximity of the HA receptor binding domain. It is possible that the mutations in the HA gene, such as R220G, may achieve a balance between the HA and NA protein in the NAI resistant virus. The exact mechanism of this phenomenon would require further investigation.

The R292K mutant virus exhibited a high level of resistance to oseltamivir with the IC_{50} -fold change >1000 , but the replication of the variant can be partially inhibited under a high concentration of zanamivir or peramivir, a finding similar to previous reports.^{9,20–22} Among available NA inhibitors, zanamivir showed the best inhibitory effect against the R292K variant with the lowest IC_{50} value in enzyme-based or cell-based assays. However, inhaled zanamivir is currently not recommended for H7N9 patients who may have impaired lung function and there are not sufficient data regarding the use of inhaled zanamivir in patients with severe influenza disease. Whether intravenous zanamivir could control an oseltamivir-resistant virus should be further tested in animal models and clinical investigations.

Notably, non-NAIs, including inhibitors for viral polymerase activity (ribavirin and T705), largely retained their effectiveness against the R292K variant. However, for NT-300, known as an inhibitor to HA glycoprotein maturation, an over 10-fold increase of IC_{50} to the R292K variant is speculated to be caused by an HA R220G mutation, although

Table 2 Cell culture-based IC_{50} values of NAIs and non-NAIs

	IC_{50} value (μ M) [mean (95% CI)]					
	Oseltamivir carboxylate	Zanamivir	Peramivir	T-705	Ribavirin	NT-300
SH5190	0.37 (0.30–0.47)	0.51 (0.31–0.83)	0.07 (0.05–0.10)	3.10 (1.67–5.76)	3.32 (1.61–6.83)	0.12 (0.07–0.21)
SH5190 R292K	>1000	33.5 (7.35–152.6)	898 (N.A.)	6.26 (4.96–7.90)	7.43 (7.80–9.52)	1.60 (1.14–2.23)

Abbreviation: N.A., not available.

Table 3 Combination Index for selected NAIs and non-NAIs against R292K-resistant H7N9 virus

Drug A	Drug B	CI at IC ₅₀	CI at IC ₉₀
NT-300	Zanamivir	3.253	1.484
Ribavirin		4.553	3.552
T-705		2.115	0.717
NT-300	Peramivir	2.700	0.700
Ribavirin		1.266	0.444
T-705		2.050	3.708
NT-300	Ribavirin	0.875	1.611
T-705	Ribavirin	0.732	0.578
T-705	NT-300	1.067	1.055

CI values that are less than 1 are in boldface.

no experimental evidence is available. Further mouse studies should be performed to determine whether these non-NAIs could be effective against H7N9 viruses even when administered post infection because antiviral treatment is often delayed in infected patients.

Although significant synergism is found against the wild-type virus by combining zanamivir/peramivir and non-NAIs, these regimens generally did not exhibit a synergistic effect against the R292K virus. We suspect that the high resistance of the R292K virus against NAIs greatly attenuated the synergism of combining zanamivir/peramivir and non-NAIs especially at median IC₅₀. Importantly, we observed that T-705+ribavirin constituted a moderate synergistic pair that cooperatively restricted viral growth in the cell culture model. Further animal experiments are needed to further corroborate its therapeutic advantage by utilizing the scheme designed by Chou¹⁴ for assessing drug synergism *in vivo*.

Apart from its drug sensitivity profile, the *in vivo* fitness of the R292K mutant virus is also of scientific importance. A number of publications have addressed this issue using various viral isolates or recombinant viruses in different animal models.^{19,21–23} The main findings were summarized in Table 4. Watanabe *et al.*¹⁹ generated a recombinant Anhui1 virus containing a Shanghai1 NA segment. Although not explicitly stated, the engineered mutant virus exhibited a lower titer in infected mouse lung than its wild-type counterpart at both 10³ and 10⁴ PFU dosages. Alleviated weight loss was also observed after infection with a mutant virus (10⁴ PFU inoculation). However, recombinant Shanghai1 (292K) and Shanghai1 with Anhui1 NA (292R) generated by Rong *et al.*²¹ showed comparable virulence in mice and aerosol transmission rate in guinea pigs. Marjuki *et al.*²² observed similar results using either Shanghai1 wild-type and R292K or Taiwan1 wild-type and R292K viruses. However, they found the HA of the Shanghai1R292K virus had a mixture of 151A/S and 209G/E (2013 H7 numbering), while that of the Taiwan1 mutant virus possesses a D340G substitution. Lastly, in an attempt to evaluate the pathogenicity and transmission potential of the R292K variant in a model closest to human infection, the Shanghai1 MUT-6 virus, which had 94% of 292K and 6% of 292R, was inoculated in ferrets and transmitted via direct and respiratory droplet contact. Quantitative analysis of the wild-type and the R292K variant during the course of transmission revealed that, although the R292K mutant had transmission potential, the mutant virus was outcompeted by the wild-type in the upper respiratory tract of inoculated donors and transmitted ferrets, which was suggestive of a competitive fitness loss.²³

In the current study, we observed that, although both viruses exhibited similar growth kinetics in MDCK cells, mice inoculated with the R292K variant showed delayed weight loss, lower viral loads in the lung

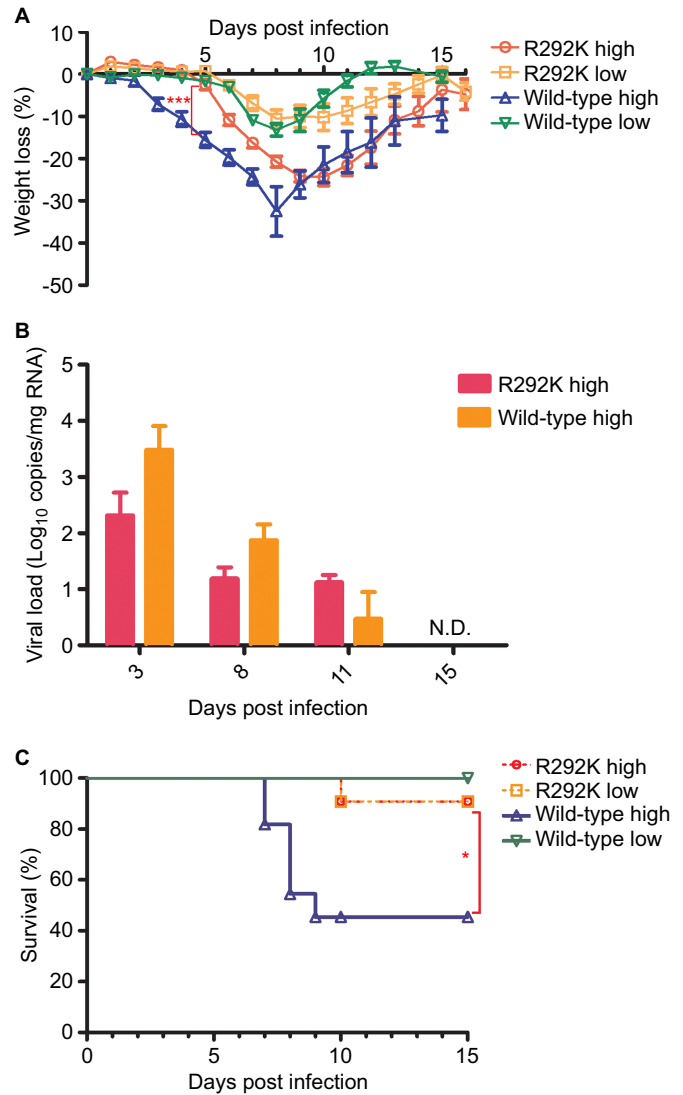


Figure 5 Pathogenicity of the H7N9 wild-type and the R292K variant in the mouse model. C57BL/6 mice ($n=11$ per group) were infected with 10⁵ (high dose) or 10³ (low dose) PFU of either the wild-type virus or the R292K variant. The mean \pm SEM of mouse weight changes (%) were recorded daily for 15 days (A); viral loads (influenza A virus HA gene copy numbers) in mouse lungs collected on days 3, 8 and 11 post infection in high-dose groups were quantified using real-time one-step qRT-PCR and expressed as mean \pm SEM of log₁₀ copy number. (B); mouse survivals after inoculation with the wild-type or the R292K variant at different doses were recorded and plotted (C). N.D. not detectable. These experiments were performed twice.

at day 3 post inoculation, milder pathological changes and greater survival rates. A number of factors may cause this discrepancy, including binding avidity to α -2,3-linked and α -2,6-linked sialic acid, cell tropism and adaptation, innate and adaptive immune response in mice. The compromised pathogenicity *in vivo* is attributed to the combined NA R292K and HA R220G mutations. It is possible that the reduced NA activity caused by the R292K mutation is responsible for the reduced fitness. However, the R220G mutation, which resides in the proximity of the HA receptor binding domain, might also contribute to compromised fitness in mice. Further study is needed to clarify the role of the HA R220G mutation on receptor binding activity and *in vivo* fitness.

The lack of concordance on the *in vivo* fitness of the R292K variant is reminiscent of the literature on the fitness of the H274Y mutation in 2009 H1N1 pandemic viruses.²⁴ Indeed, the viral strains and

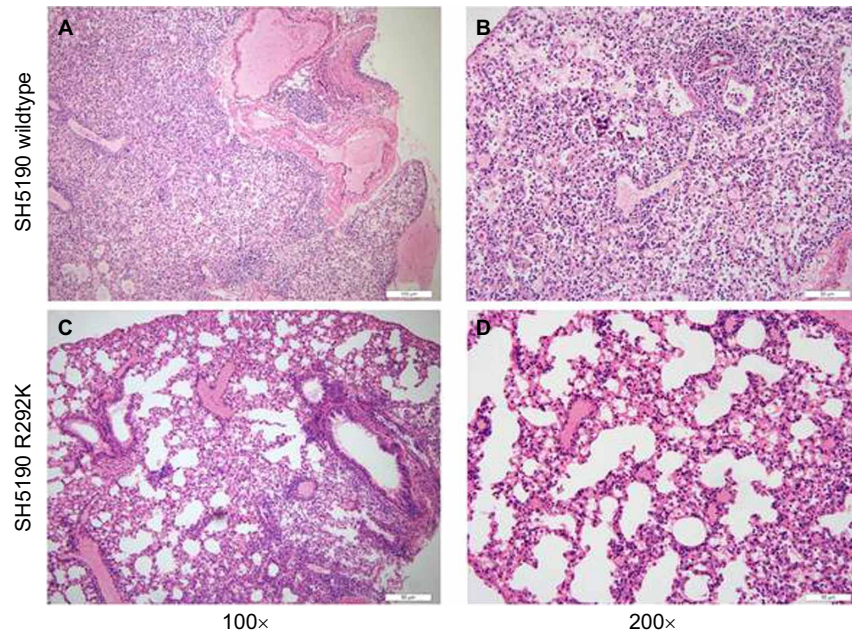


Figure 6 Hematoxylin and eosin staining of lung tissues collected on the eighth day after infection with high-dose R292K mutant virus (**A**: $\times 100$ magnification, **B**: $\times 200$ magnification) and wild-type (**C**: $\times 100$ magnification, **D**: $\times 200$ magnification).

Table 4 Fitness of R292K mutant H7N9 influenza viruses in experimental models

Resistant and sensitive virus pairs	NA mutation ^a	Mutations in other segments	Animal model	Pathogenicity	Direct transmission	Aerosol transmission	Ref
rAnhui/1:SH1-NA/ and Anhui/1	R292K, G39S	Not available	Mice	WT>R	ND	ND	19
rSH/1 and rSH/1:Anhui1-NA	R292K, S39G	Not available	Mice and guinea pigs	WT=R	ND	WT=R	21
SH1 R292K and SH1	R292K,	HA mixed 151A/S and 209G/E ^b	Mice	WT=R	ND	ND	22
TW1 R292K and TW1	R292K,	HA D340G ^b	Mice	WT=R	ND	ND	22
SH1 MUT-6 ^c	94% 292K, 6% 292R	PB1 Q687R	Ferrets	R outgrown by WT	R outgrown by WT	R outgrown by WT	23
SH5190 R292K and SH5190	R292K	HA:R220G ^d	Mice	WT>R	ND	ND	

Abbreviations: ND, not determined; r, recombinant; R, neuraminidase inhibitor-resistant virus; WT, wild-type.

^a N2 numbering.

^b 2013 H7 numbering.

^c SH1 MUT-6 had a mixed 292R/K population.

^d H3 numbering.

experimental conditions have a profound influence on the results. For H7N9 viruses, the use of Shanghai1 or Anhui1-like viruses, which differ by seven amino acids in the HA segment, can cause a significant difference. In addition, mutations other than NA 292, which may cause a compensatory effect, could also significantly affect the final readout.

Taken together, we report here the isolation and characterization of the R292K variant from a clinical specimen derived from an H7N9 fatal case of the Anhui1 lineage. It has highly reduced susceptibility to oseltamivir and reduced susceptibility to zanamivir/peramivir, but largely retained sensitivity to non-NAIs (favipiravir, nitazoxanide and ribavirin). The combination of favipiravir and ribavirin may synergistically restrict the spread of the R292K variant and needs to be tested in animal models. The reduced pathogenicity of the R292K variant suggests that it is partially compromised *in vivo*, at least in the mouse model. The *in vivo* fitness of the R292K H7N9 variant virus

should be further assessed with genetically well-characterized pairs of viruses and most desirably, with competitive fitness experiments. Resistant variants should be closely monitored, both genotypically and phenotypically, in H7N9 patients under NAI treatment.

ACKNOWLEDGEMENTS

This research was supported by the National Megaprojects of China for Infectious Disease (2012ZX10004211 and 2014ZX10004002-003-004), National Natural Science Foundation of China (81341004), Ministry of Science and Technology (KJYJ-2013-01-01) and Shanghai Municipal Health and Family Planning Commission (2013QLG002).

1 Gao R, Cao B, Hu Y *et al*. Human infection with a novel avian-origin influenza A (H7N9) virus. *N Engl J Med* 2013; **368**: 1888–1897.

- 2 Lam TT-Y, Wang J, Shen Y *et al*. The genesis and source of the H7N9 influenza viruses causing human infections in China. *Nature* 2013; **502**: 241–244.
- 3 Wu A, Su C, Wang D *et al*. Sequential reassortments underlie diverse influenza H7N9 genotypes in China. *Cell Host Microbe* 2013; **14**: 446–452.
- 4 Liu D, Shi W, Shi Y *et al*. Origin and diversity of novel avian influenza A H7N9 viruses causing human infection: phylogenetic, structural, and coalescent analyses. *Lancet* 2013; **381**: 1926–1932.
- 5 Wang D, Yang L, Gao R *et al*. Genetic tuning of the novel avian influenza A(H7N9) virus during interspecies transmission, China, 2013. *Euro Surveill* 2014; **19**. pii: 20836
- 6 Ren L, Yu X, Zhao B *et al*. Infection with possible precursor of avian influenza A(H7N9) virus in a child, China, 2013. *Emerg Infect Dis* 2014; **20**: 1362–1365.
- 7 McKimm-Breschkin JL. Influenza neuraminidase inhibitors: antiviral action and mechanisms of resistance. *Influenza Other Respir Viruses* 2013; **7**(Suppl 1): 25–36.
- 8 Yen HL, Herlocher LM, Hoffmann E *et al*. Neuraminidase inhibitor-resistant influenza viruses may differ substantially in fitness and transmissibility. *Antimicrob Agents Chemother* 2005; **49**: 4075–4084.
- 9 Yen HL, McKimm-Breschkin JL, Choy KT *et al*. Resistance to neuraminidase inhibitors conferred by an R292K mutation in a human influenza virus H7N9 isolate can be masked by a mixed R/K viral population. *mBio* 2013; **4**. pii: e00396-13
- 10 Hu Y, Lu S, Song Z *et al*. Association between adverse clinical outcome in human disease caused by novel influenza A H7N9 virus and sustained viral shedding and emergence of antiviral resistance. *Lancet* 2013; **381**: 2273–2279.
- 11 Lin PH, Chao TL, Kuo SW *et al*. Virological, serological, and antiviral studies in an imported human case of avian influenza A(H7N9) virus in Taiwan. *Clin Infect Dis* 2014; **58**: 242–246.
- 12 Kageyama T, Fujisaki S, Takashita E *et al*. Genetic analysis of novel avian A(H7N9) influenza viruses isolated from patients in China, February to April 2013. *Euro Surveill* 2013; **18**: 20453.
- 13 Wang W, Song Z, Guan W *et al*. PCR for detection of oseltamivir resistance mutation in influenza A(H7N9) virus. *Emerg Infect Dis* 2014; **20**: 847–849.
- 14 Chou TC. Theoretical basis, experimental design, and computerized simulation of synergism and antagonism in drug combination studies. *Pharmacol Rev* 2006; **58**: 621–681.
- 15 Chou TC. Drug combination studies and their synergy quantification using the Chou-Talalay method. *Cancer Res* 2010; **70**: 440–446.
- 16 Zhu Z, Yang Y, Feng Y *et al*. Infection of inbred BALB/c and C57BL/6 and outbred Institute of Cancer Research mice with the emerging H7N9 avian influenza virus. *Emerg Microbes Infect* 2013; **2**: e50.
- 17 Gao HN, Lu HZ, Cao B *et al*. Clinical findings in 111 cases of influenza A (H7N9) virus infection. *N Engl J Med* 2013; **368**: 2277–2285.
- 18 Liu X, Li T, Zhen YF, Wong KW, Lu SH, Lu HZ. Poor responses to oseltamivir treatment in a patient with influenza a (H7N9) infection. *Emerg Microbes Infect* 2013; **2**: e27.
- 19 Watanabe T, Kiso M, Fukuyama S *et al*. Characterization of H7N9 influenza A viruses isolated from humans. *Nature* 2013; **501**: 551–555.
- 20 Sleeman K, Guo Z, Barnes J, Shaw M, Stevens J, Gubareva LV. R292K substitution and drug susceptibility of influenza A(H7N9) viruses. *Emerg Infect Dis* 2013; **19**: 1521–1524.
- 21 Rong H, Schmolke M, Leyva-Grado VH *et al*. Influenza A(H7N9) virus gains neuraminidase inhibitor resistance without loss of *in vivo* virulence or transmissibility. *Nat Commun* 2013; **4**: 2854.
- 22 Marjuki H, Mishin VP, Chesnokov AP *et al*. An investigational antiviral drug, DAS181, effectively inhibits replication of zoonotic influenza A virus subtype H7N9 and protects mice from lethality. *J Infect Dis* 2014; **210**: 435–440.
- 23 Yen HL, Zhou J, Choy KT *et al*. The R292K mutation that confers resistance to neuraminidase inhibitors leads to competitive fitness loss of A/Shanghai/1/2013 (H7N9) influenza virus in ferrets. *J Infect Dis* 2014; June 20. doi:10.1093/infdis/jiu353.
- 24 Baranovich T, Webster RG, Govorkova EA. Fitness of neuraminidase inhibitor-resistant influenza A viruses. *Curr Opin Virol* 2011; **1**: 574–581.



This work is licensed under a Creative Commons Attribution-NonCommercial-ShareAlike 3.0 Unported License. The images or other third party material in this article are included in the article's Creative Commons license, unless indicated otherwise in the credit line; if the material is not included under the Creative Commons license, users will need to obtain permission from the license holder to reproduce the material. To view a copy of this license, visit <http://creativecommons.org/licenses/by-nc-sa/3.0/>

Supplementary Information for this article can be found on *Emerging Microbes & Infections'* website (<http://www.nature.com/emi/>)